

# Diffusion in crowded colloids of particles cyclically changing their shapes: A model for bacterial cytoplasm

Yuki Koyano

*Department of Physics, Tohoku University, 6-3, Aoba, Aramaki, Aoba-ku, Sendai 980-8578, Japan*

Hiroyuki Kitahata

*Department of Physics, Chiba University, 1-33 Yayoi-cho, Inage-ku, Chiba 263-8522, Japan*

Alexander S. Mikhailov

*WPI Nano Life Science Institute, Kanazawa University, Kakuma-machi, Kanazawa 920-1192, Japan and  
Abteilung Physikalische Chemie, Fritz-Haber-Institut der Max-Planck-Gesellschaft, Faradayweg 4-6, 14195 Berlin, Germany*

Crowded colloids of particles that cyclically change their shapes, but do not propel themselves, can be viewed as an idealization of bacterial cytoplasm. Our simulations for a proposed model of oscillating dumbbells, performed at the parameter values characteristic for active proteins in the cytoplasm, reveal a dramatic effect of non-equilibrium conformational activity on diffusion and structural relaxation phenomena in such systems. As we find, while passive crowded colloids behave as glass-like systems, they become fluidized when non-equilibrium conformational activity is turned on. This agrees with experimental results of *in vivo* optical tracking of genetically engineered probe particles in bacterial cells where metabolism-induced fluidization of the cytoplasm was observed.

## I. INTRODUCTION

Typical examples of active colloids are provided by populations of microscopic particles or biological organisms that are able to propel themselves [1]. It has been experimentally demonstrated that diffusion in the colonies of swimming bacteria can be strongly enhanced [2] and the theory for this effect is available too (see, e.g., [3]). Active colloids can however be also formed at nanoscales by macromolecules that cyclically change their shapes under energy supply. Specifically, the cytoplasm of bacterial cells is known to represent a solution of conformationally active proteins, such as enzymes, motors and molecular machines [4]. This solution can be so crowded that the macromolecules almost touch one another within it.

The estimates reveal that, in contrast to biological microorganisms, single active proteins cannot usually propel themselves [5]: the conformational motions within their turnover cycles are only weakly non-reciprocal and the resulting propulsion forces are too small [7, 8]. Therefore, such systems constitute a special class of active colloids, where individual particles are repeatedly changing their shapes, but do not swim.

Even in absence of self-propulsion, persistent energy-driven conformational changes in macromolecules create non-thermal fluctuating hydrodynamical flows around them. It has been already shown that, because passive tracer particles are advected by such fluctuating flows, their diffusion can become enhanced [9–11]. However, the analysis has so far been limited to dilute systems and therefore its results are not directly applicable to highly crowded colloids, such as the cytoplasm.

At sufficiently large volume ratios, passive colloids are known to have glass-like properties, manifested by slow relaxation, subdiffusion, and non-ergodicity (see, e.g., re-

view [12]). *In vivo* experiments [13] on optical tracking of particles inside bacterial or yeast cells have been performed - with a surprising result that, at least for the probe particles with relatively large sizes, such glass behavior is only characteristic under starvation conditions or in absence of the chemical fuel, such as ATP. The metabolism fluidizes the cytoplasm, leading to recovery of classical transport properties for it.

In this Letter, we propose an idealized model of oscillatory active colloids where the activity level and the rate of energy supply can be controlled. The individual particles forming the considered colloid are active dimers, or *dumbbells* [9, 14]. It is known that such active dimers reproduce, in an approximate way, the mechanochemical activity in real enzymes and protein machines [15]. Moreover, they have been already employed [16] in large-scale hydrodynamic simulations of the colloids (but still under less crowded conditions where glass effects are not seen). In contrast to the previous publications [9, 11, 15, 16], our dumbbells are however further simplified: we assume that the natural length of the elastic spring that connects two beads in a dumbbell is periodically varied with time. In the present version, the system does not include special probe particles of controlled size and random motions of individual dumbbells in the colloid are instead traced.

The principal result of our model simulations is that diffusion in the colloid is strongly enhanced when shape oscillations of its constituting particles are turned on. This suggests that non-thermal noise, caused by non-equilibrium conformational activity in the system, plays a dominant role in determining the mobility of particles within it. We also find that, in the active system, classical diffusion takes places. In contrast to this, the passive colloid has characteristic properties of a glass.

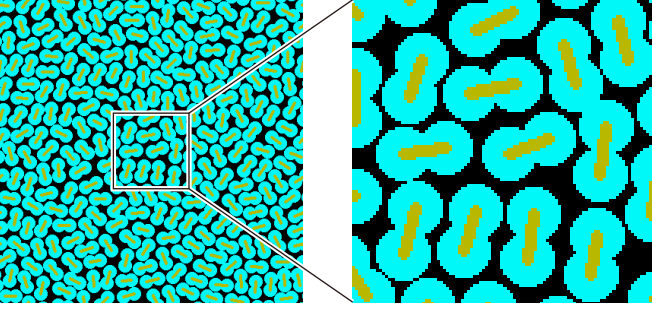


FIG. 1. The crowded colloid of oscillating dumbbells.

## II. THE MODEL

Enzymes are single-protein catalysts that convert substrate(s) into product(s) in each turnover cycle. In most enzymes, the cycles are accompanied by internal mechanochemical motions, i.e. by repeated changes in the conformation of the protein. Biological molecular motors and machines are also enzymes, with the only difference that mechanochemical motions are employed by them to manipulate other macromolecules or to produce mechanical work. To do this, chemical energy supplied with the substrate (often, ATP) is used. The bacterial cytoplasm is essentially a densely packed colloid of active proteins that are repeatedly changing their shapes.

Typically, mechanochemically active enzymes have a domain structure and their ligand-induced internal motions consist of the changes in distances between the domains and mutual orientation of them. Principal properties can be already reproduced in a simple active dimer model of an enzyme (see review [15]).

In the model, an enzyme protein is viewed as consisting of two beads (domains) connected by an elastic spring. The natural length of this spring depends on the ligand state of the enzyme: it is longer in absence of a ligand, but gets shorter after the substrate-enzyme and product-enzyme complexes are formed, returning to the original longer length after the product release. Thus, an enzyme behaves as a mechanochemical oscillator that undergoes an elongation and a contraction in each turnover cycle [15].

This model has been successfully used to investigate collective hydrodynamic effects in numerical simulations for large populations of catalytically active enzymes [16]. In our study, it will be however further simplified: we will not explicitly consider the ligand states and chemical transitions between them. Instead, it shall be just assumed that the natural length of the spring connecting two beads in a dimer is periodically (with some additional random drift) changing with time. Physically, the modulation period should be considered as corresponding to the turnover time of an enzyme.

Explicitly, we assume that the natural length  $\ell_i$  of

dumbbell  $i$  oscillates with time as

$$\ell_i(t) = \ell_0 + \ell_1 \sin \psi_i(t), \quad (1)$$

where the oscillation phase satisfies the equation

$$\frac{d\psi_i}{dt} = \omega_i + \zeta_i(t). \quad (2)$$

Here,  $\omega_i$  is the mean oscillation frequency and  $\zeta_i(t)$  is the internal noise that takes into account stochastic variations in cycle times. This Gaussian noise is delta-correlated in time and independent for different dumbbells,

$$\langle \zeta_i(t) \zeta_j(s) \rangle = 2\eta \delta_{ij} \delta(t-s). \quad (3)$$

The parameter  $\eta$  controls the characteristic coherence time for oscillations of the shape. Below we assume that all dumbbells are identical and have the same oscillation frequency  $\omega$ .

Thus, the time-dependent elastic energy of dumbbell  $i$  is

$$E_i(t) = \frac{1}{2}k \left( r_{12}^{(i)} - \ell_i(t) \right)^2, \quad (4)$$

where  $k$  is the stiffness of the internal spring and  $r_{12}^{(i)} = \left| \mathbf{r}_i^{(1)} - \mathbf{r}_i^{(2)} \right|$  is the distance between the first and the second beads in the dumbbell  $i$ .

The considered colloid consists of  $N$  dumbbells located within a volume of linear length  $L$  (periodic boundary conditions are used). Any two beads belonging to different dumbbells are interacting via a soft repulsive potential

$$u(r) = \begin{cases} u_0 (R-r)^2, & r \leq R \\ 0, & r > R \end{cases} \quad (5)$$

where  $r$  is the distance between the beads. Here, the parameter  $u_0$  specifies the repulsion strength and  $R$  is the distance between the particles at which the repulsion begins.

It can be expected that, for crowded colloids, direct collisions between the particles shall dominate over hydrodynamic interactions between them. Therefore, we shall assume that motion of the beads is governed by stochastic Langevin dynamics, i.e. that the velocity of the bead  $n = 1, 2$  in dumbbell  $i$  is

$$\frac{d\mathbf{r}_i^{(n)}}{dt} = -\mu \frac{\partial E_i}{\partial \mathbf{r}_i^{(n)}} - \mu \frac{\partial U_i}{\partial \mathbf{r}_i^{(n)}} + \boldsymbol{\xi}_i^{(n)}(t). \quad (6)$$

Here  $\mu$  is the mobility of the beads and

$$U_i(\mathbf{r}) = \sum_{j \neq i} \sum_{m=1,2} u \left( \left| \mathbf{r}_j^{(m)} - \mathbf{r} \right| - R \right) \quad (7)$$

represents the potential experienced at position  $\mathbf{r}$  by a bead of the dumbbell  $i$ , resulting from repulsive interactions with the beads of all other dumbbells (note that

there is no repulsion between the two beads in the same dumbbell). Moreover,  $\xi_i^{(n)}(t)$  is the Gaussian thermal noise acting on the bead  $n$  in the dumbbell  $i$ . Its correlation functions are

$$\langle \xi_{i,\alpha}^{(m)}(t) \xi_{j,\beta}^{(n)}(s) \rangle = 2\mu k_B T \delta_{mn} \delta_{ij} \delta_{\alpha\beta} \delta(t-s), \quad (8)$$

where  $T$  is the temperature,  $k_B$  is the Boltzmann constant, and  $\alpha, \beta = (x, y, z)$  in 3D or  $\alpha, \beta = (x, y)$  in 2D.

It is convenient to measure all lengths in units of the repulsion interaction radius  $R$  and the time in units of the relaxation time  $\tau = (\mu k)^{-1}$  of the dumbbell. On the considered molecular scales, a convenient unit of energy is the thermal energy  $k_B T$ .

After rescaling, the model is characterized by a set of dimensionless parameters:

$$\begin{aligned} a_0 &= \frac{\ell_0}{R}, & a_1 &= \frac{\ell_1}{R}, & \Omega &= \omega\tau, \\ Y &= \eta\tau, & \kappa &= \frac{kR^2}{k_B T}, & \nu &= \frac{u_0 R^2}{k_B T}. \end{aligned} \quad (9)$$

Through periodic modulation of the natural length of the spring connecting two beads, energy is persistently supplied to a dumbbell. To estimate its mean supply rate, we can notice that it should be also the mean rate at which energy is dissipated by the dumbbell. A simple calculation yields that the energy  $\Delta E$  supplied to an active dumbbell per one oscillation period is

$$\frac{\Delta E}{k_B T} = \frac{\pi a_1^2 \kappa \Omega}{1 + \Omega^2}. \quad (10)$$

Additionally, an important parameter of the model is the fraction  $\phi$  of the total volume occupied by the dumbbells. Figure 1 shows an example of the simulated active colloid.

### III. THE CHOICE OF PARAMETERS

Depending on the parameter values, our model of an oscillatory colloid can describe various systems, including, for example, populations of biological microorganisms that cyclically change their shapes. The focus in the present study is however on the intracellular bacterial cytoplasm and, therefore, the parameters typical for it shall be used.

Protein domains, corresponding to dumbbell beads in our model, typically have the size of about 10–20 nm. They are so stiff that one domain cannot deform another and penetrate inside it. Therefore, a repulsive hard-core potential could have been a good candidate to describe repulsive interactions between them. There are however also soft electrostatic interactions between proteins that extend over a few nanometers. Additionally, a protein is surrounded by a layer of hydrated water that is soft [17]. Moreover, when a protein moves, it creates hydrodynamic flows in the solvent, pushing away

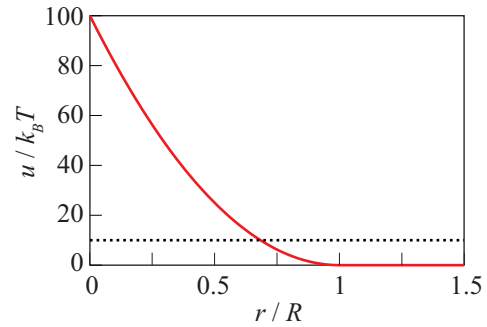


FIG. 2. Repulsive interaction potential  $u/(k_B T)$  as a function of the distance  $r/R$  between the beads from different dumbbells. The radius  $\sigma = 0.68R$ , corresponding to the potential level of  $10k_B T$  (dotted line), is chosen to define the “hard-core” size of a bead.

the neighbour proteins. Recently, non-contact effective interactions between proteins in water were analyzed by direct molecular dynamics simulations [19].

In our simple model, there is a single interaction potential (5) and hydrodynamic effects are not explicitly resolved. Nonetheless, one can interpret this potential as having a hard core and a soft interaction shell. The boundary between them can be approximately defined as a radius  $\sigma$  at which the repulsion potential becomes much larger than the thermal energy  $k_B T$ . Hence, when two beads interact, they can still penetrate one into another until the radius  $\sigma$  is reached. Because of this, one can choose  $\sigma$  as the radius of the bead.

Below, we take  $u_0 = 100k_B T$  in equation (5) and define the bead “hard-core” radius by the condition that  $u(r = \sigma) = 10k_B T$ , which yields approximately  $\sigma = 0.68R$  (see Fig. 2).

If particles of linear size  $\sigma$  are randomly distributed at the mean distance of  $d$  between them, their volume fraction is about  $\phi_{3D} = (\sigma/d)^3$  or the area fraction about  $\phi_{2D} = (\sigma/d)^2$  in the 2D case, where the numerical prefactors that depend on particle shapes are dropped. In bacteria, about 30 percent of cytosol is typically occupied by proteins [18]. Assuming that all proteins have the same size  $\sigma$  and using the above estimate, this yields the relative distance of about  $d/\sigma = 0.3^{-1/3} \simeq 1.5$  between them. If, for example,  $\sigma = 0.68R$ , this corresponds to  $d \simeq R$ , so that all neighbours of a protein would typically be located within the interaction radius from it.

In our 2D simulations, we had 246 dumbbells within the area with linear size  $L = 40R$ . Assuming that the radius of a bead is  $\sigma = 0.68R$ , this yields the area fraction of  $\phi_{2D} = 0.45$ . In a 3D system, this would have corresponded to the volume fraction of  $\phi_{3D} = 0.37$ .

The relaxation time  $\tau$  of the dumbbell should be about the characteristic slow conformational relaxation time in a protein, which is of the order of milliseconds. On the other hand, the turnover cycle time of an enzyme, corresponding in our model to the modulation period  $2\pi/\omega$ , typically takes tens of milliseconds. There-

fore, we can choose  $\Omega = 0.1$ . The initial oscillation phases will be randomly chosen for different dumbbells and weak noise with  $Y = 10^{-3}$  will be moreover included into the phase evolution equation (2).

We assume that the mean distance between the beads in the dumbbell is  $\ell_0 = 1.5R$ , so that  $a_0 = 1.5$ , and the dimensionless stiffness of the spring connecting them is  $\kappa = 100$ . The parameter  $a_1 = \ell_1/R$ , defining the amplitude of shape oscillations, has been varied from 0 (for the passive dumbbells) to 1 in our simulations. The energy supplied to our model enzyme per its single cycle is  $\Delta E = 7.8k_B T$  at  $a_1 = 0.5$  and  $\Delta E = 31.1k_B T$  at  $a_1 = 1.0$ . For comparison, the chemical energy released in the reaction of ATP hydrolysis, often powering protein machines, is about  $20k_B T$ .

#### IV. NUMERICAL SIMULATIONS

In our two-dimensional simulations, periodic boundary conditions have been used. To prepare the initial configuration, the following procedure was employed:

We started with a system where all dumbbells had a zero natural length,  $\ell_0 = 0$ , and they were regularly distributed forming a two-dimensional grid. Then, a short numerical simulation of this system over the time interval of  $100\tau$  was performed. During this simulation, system's temperature was raised 5-fold and, moreover, the natural length of dumbbell springs  $\ell_0$ , together with the modulation amplitude  $\ell_1$  were gradually increased from zero to  $\ell_0 = 1.5R$  and  $\ell_1 = a_1 R$ . The equations were then integrated over further  $100\tau$ . Configurations of particles established at the end of such preparatory simulations were used as initial conditions for the actual simulations with the duration of  $50000\tau$ .

To explore the diffusion phenomena, we traced motion of the centers of mass,  $\mathbf{p}_i = (\mathbf{r}_i^{(1)} + \mathbf{r}_i^{(2)})/2$ , for all dumbbells  $i$ . Thus, trajectories were obtained that could be further analyzed. Averaging was always performed over all 246 different dumbbells in one simulation.

Note that at very short times, corresponding to displacements of mass centers much less the mean distance between the particles, interactions between the dumbbells do not play a role. In this short-time regime, free Brownian motion of an isolated dumbbell, described by the Langevin equation (6) without the interaction terms, should be observed. For the considered system, the diffusion coefficient for an isolated dumbbell is  $D_0 = 0.005 R^2/\tau$ . At such very short times, the mean-square displacement (MSD) of a dumbbell from its initial position should be

$$\langle \Delta \mathbf{p}^2(t) \rangle = 4D_0 t. \quad (11)$$

The mean-square-displacements (MSD) of dumbbells, determined in our simulations, are shown as functions of time for different activity levels in Fig. 3. In these plots, we omit the initial short-time parts corresponding to free diffusion described above.

It can be noticed that the dependences in Fig. 3 have the form characteristic for colloidal glasses [12, 20]. They can be analyzed by fitting them to power laws  $t^\beta$ . As seen in Fig. 3, one gets different exponents  $\beta_-$  and  $\beta_+$  in the intermediate- and long-time regimes. For the passive system ( $a_1 = 0$ ), we have the exponents  $\beta_- = 0.55$  and  $\beta_+ = 0.92$  with  $t_{\text{cross}} = 336\tau$ . At the activity level of  $a_1 = 0.5$ , the exponents are increased to  $\beta_- = 0.61$  and  $\beta_+ = 0.97$  with  $t_{\text{cross}} = 206\tau$ . At the highest considered activity level of  $a_1 = 1$ , we obtain  $\beta_- = 0.75$  and  $\beta_+ = 0.99$  with  $t_{\text{cross}} = 121\tau$ .

Thus, classical free diffusion (11) with the exponent  $\beta = 1$  at very short times (not shown) is replaced by subdiffusion with the exponents  $\beta_-$  ranging between 0.55 and 0.75 at the times less than  $t_{\text{cross}}$ . At the longer times, classical diffusion is however recovered since the determined exponents  $\beta_+$  are close to one. The diffusion coefficient  $D$  at such long times is however smaller than  $D_0$ , indicating that diffusion in the colloid becomes suppressed.

Both the suppression of diffusion at long times and the observed subdiffusion at intermediate times are the typical glass effect. They suggest that *caging* of particles takes place [12]. The free diffusive motion of a particle is blocked by other particles surrounding it and forming a cage. Displacements over large distances are only possible if, by a rare fluctuation, the particle were able to escape from its cage.

The dependence of the long-time diffusion coefficient of particles on the activity level  $a_1$  is shown in Fig. 4. We see that diffusion becomes enhanced when non-equilibrium conformational activity of dumbbells is introduced and gradually increased. Alternatively, it can be said that suppression of diffusion with respect to that for free particles becomes then less strong. Furthermore, it can be noticed that the subdiffusion exponent  $\beta_-$  gets larger at higher activity levels and the classical diffusion regime sets on earlier (i.e., at the shorter cross-over times  $t_{\text{cross}}$ ) with an increase in the parameter  $a_1$ .

Similar behavior is observed in equilibrium colloids when the volume or area fractions of particles are decreased; it corresponds to a transition from the glass to the fluid phase [12, 20]. The above results suggest that an effective fluidization of a colloid can also take place because of the non-equilibrium conformational activity of the particles forming it.

To further explore this conjecture, structural relaxation in the model has been numerically analyzed. To do this, we have determined the scattering function

$$F_2(\mathbf{k}, t) = \frac{1}{N} \left\langle \sum_i e^{i\mathbf{k} \cdot (\mathbf{p}_i(t) - \mathbf{p}_i(0))} \right\rangle. \quad (12)$$

Because of the isotropy of the system, this function depends only on  $k = |\mathbf{k}|$ .

The determined functions  $F_2(k_{\text{max}}, t)$  are shown for three different activity levels in Fig. 5a. Here,  $k_{\text{max}} = 2\pi/b$  where  $b = L/N^{1/2}$  is the mean distance between the

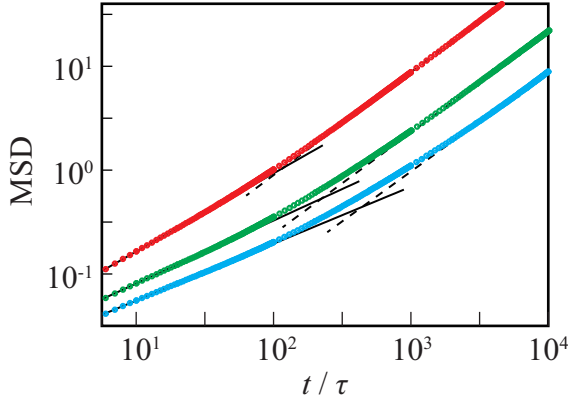


FIG. 3. Dependences of the mean-square-displacement (MSD) of particles (in units of  $R^2$ ) on dimensionless time  $t/\tau$  for systems with passive ( $a_1 = 0$ , blue) and active ( $a_1 = 0.5$ , green, and  $a_1 = 1.0$ , red) dumbbells. Solid and dashed lines show power-law fits with the exponents  $\beta_-$  and  $\beta_+$  for each system. The crossover times  $t_{\text{cross}}$  correspond to intersections of these lines..

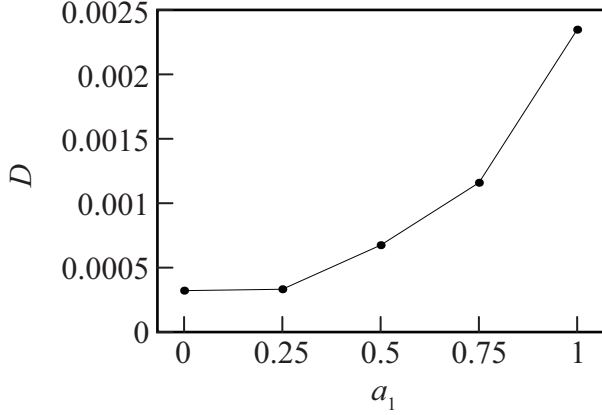


FIG. 4. Long-time diffusion coefficients of particles (in units of  $R^2/\tau$ ) at different activity levels  $a_1$ . At the same parameter values, the diffusion coefficient for a single free dumbbell is  $D_0 = 0.005 R^2/\tau$

dumbbells. The structural relaxation time  $\tau_\alpha$  is defined [12] by the equation

$$F_2(k_{\text{max}}, \tau_\alpha) = \frac{1}{e}. \quad (13)$$

The dependence of  $\tau_\alpha$  on the activity level  $a_1$  is displayed in Fig. 5b.

As we see, the structural relaxation gets much faster when the non-equilibrium conformational activity in the particles takes place. It decreases by an order of magnitude in comparison to the passive colloid ( $a_1 = 0$ ) when  $a_1 = 1.0$ .

To further explore statistical properties of trajectories, we determined statistical distributions of displacements  $|\Delta \rho|$  within a given time  $\Delta t$ . For classical diffusion, such

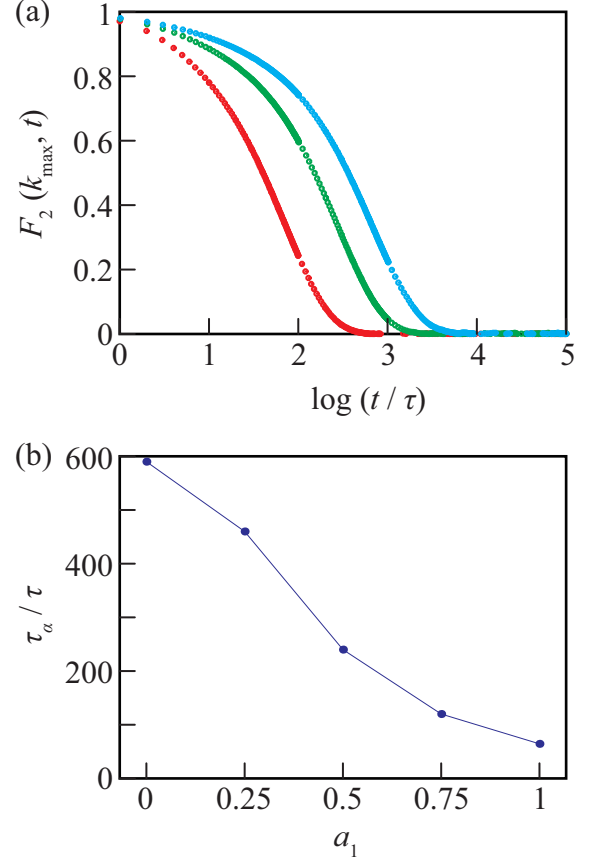


FIG. 5. (a) Scattering functions  $F_2(k_{\text{max}}, t)$  at  $a_1 = 0$  (blue), 0.5 (green), and 1.0 (red). (b) Structural relaxation times  $\tau_\alpha$  at various activity levels  $a_1$ .

distributions should be

$$p(|\Delta \rho|) \propto |\Delta \rho| \exp\left(-\frac{|\Delta \rho|^2}{2Dt}\right). \quad (14)$$

Therefore, the ratio  $p(|\Delta \rho|)/|\Delta \rho|$  has then the Gaussian form.

In Fig. 6, we show the normalized histograms where the frequencies of displacements at three activity levels within time  $\Delta t = 1000\tau$  are divided by  $|\Delta \rho|$ . Additionally, this figure shows the fits of such distributions to the Gaussian form. It can be noticed that, for a passive colloid, the distribution deviates from the Gaussian dependence for large displacements  $\Delta \rho$ . When non-equilibrium conformational activity is switched on, the deviations become smaller and they practically disappear at  $a_1 = 1.0$ .

To quantitatively characterize the deviations, the non-Gaussianity coefficient

$$\alpha_d = \frac{\langle |\Delta \rho|^4 \rangle}{\zeta_d \langle |\Delta \rho|^2 \rangle^2} - 1 \quad (15)$$

is introduced, where  $\zeta_d = 1 + 2/d$  and  $d$  is the dimensionality of the system. This coefficient vanishes in the

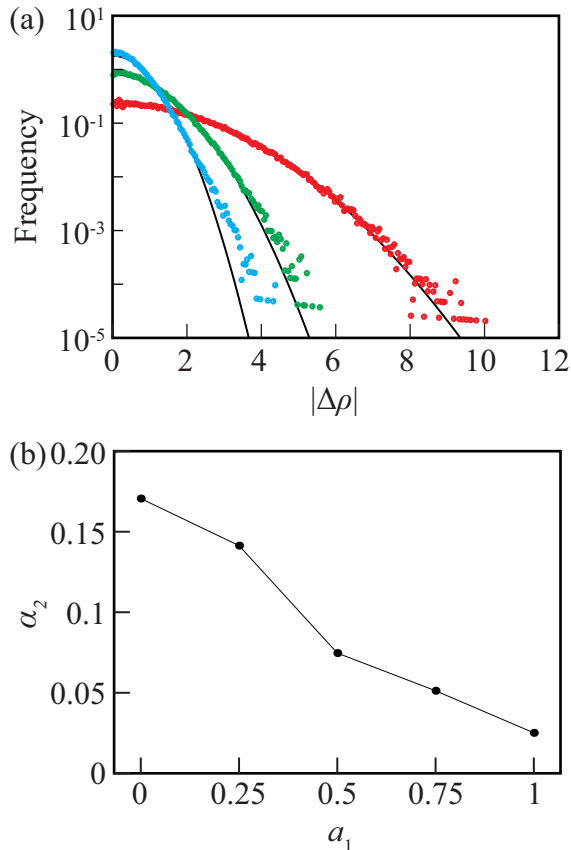


FIG. 6. (a) Normalized distributions of displacements (see the text) within the time interval  $\Delta t = 1000\tau$  for passive ( $a_1 = 0$ , blue) and active ( $a_1 = 0.5$ , green, and  $a_1 = 1.0$ , red) dumbbells. Solid curves are fits to the Gaussian form. (b) Non-Gaussianity coefficients  $\alpha_2$  at different activity levels  $a_1$  for  $\Delta t = 1000\tau$ .

Gaussian case. The coefficients  $\alpha_2$  at different activity levels are shown in Fig. 6. One can see that such coefficients decrease at higher activity levels, thus further supporting our conclusion that fluidization of the system takes place.

## V. DISCUSSION AND CONCLUSIONS

In this Letter, we have proposed a simple model of a colloid consisting of active particles that reciprocally change their shapes. This model can be used to study characteristic properties of bacterial and yeast cytoplasm that represents a crowded solution of active proteins, enzymes and molecular machines, whose conformations are cyclically changed. The parameters of the model could be chosen in such a way that the conditions typical for living cells are approximately reproduced. The rate of energy supply to such macromolecular colloid could be varied in our simulations, allowing us to investigate how the diffusion phenomena are changed when deviations from

thermal equilibrium are gradually increased. Numerical simulations for this model have been performed.

Our principal result is that, already at the rates of energy supply of about  $10k_B T$  per a particle within its conformational oscillation cycle, kinetic properties of the system become dramatically changed. While the passive colloid behaves essentially as a glass, the glass properties fade away and tend to disappear as the non-equilibrium conformational activity is increased. Thus, the diffusion of particles becomes enhanced by an order of magnitude and the structural relaxation time is greatly shortened.

In an equilibrium colloid, such changes would have occurred when the volume fraction of particles is reduced and system becomes fluidized. Therefore, our results suggest that the cytoplasm, having glass-like properties in absence of metabolism, can become effectively fluidized when the energy supply is turned on and the shapes of its constituting particles cyclically change.

Previously, a similar conclusion has been made based on the data of the *in vivo* tracking studies in biological cells [13]. In these experiments, positions of fluorescent genetically engineered particles with the sizes varying from 50 nm to 150 nm were optically tracked in bacteria *E. coli* and in yeast cells, and the trajectory data was statistically analyzed. Generally, it was found that classical diffusion phenomena were characteristic in presence of metabolism. However, diffusion was much slowed down and glass properties were observed under starvation conditions or when ATP, i.e. the chemical fuel, was depleted in bacterial or yeast cells.

As stressed by the authors of the publication [13], the effects depended however strongly on the size of the engineered tracer particles, with the glass-like properties in absence of metabolism much less pronounced for the probe particles of the smallest 50 nm size. In our investigation, additional tracer particles of controlled size were not introduced and, so far, only random trajectories of individual dumbbells forming the colloid were traced. A dumbbell corresponds to a protein and the typical protein size would be several times smaller than 50 nm.

Therefore, the results of our numerical simulations cannot be directly compared with the experimental data [13]. Nonetheless, some comments can still be made. According to a detailed statistical analysis [21], cages in colloidal glasses are characterized by a hierarchical onion-like structure, with the smaller ones enclosed within the larger ones. If a smaller cage is destroyed and the particle escapes from it, it may still stay confined within the larger cage. Moreover, characteristic times of diffusion processes get progressively increased with the cage size, following a self-similarity law [21].

It seems natural to assume that large probe particle can be only confined within the cages of the respective large size. Moreover, one might expect that the diffusion phenomena for such probe particles would be qualitatively the same as for the smaller particles forming a colloid, but it will be scaled up in time. Thus, a cross-over from subdiffusion to classical diffusion would occur at

the mean-square-displacements about the square of the probe particle size, i.e. the cross-over time  $t_{\text{cross}}$  in Fig. 3 will increase with this size. In the experiments [13], only the displacements within relatively long times could be observed. For the smaller probe particles, the observation times could have been closer to  $t_{\text{cross}}$  and thus the glass effects could have been more weak.

Dense colloids are characterized by rich cooperative phenomena, such as dynamic heterogeneity, (see [12, 20, 21]) and these phenomena could also be experimentally investigated for bacterial cytoplasm [13]. The cooperative effects are however known to strongly depend on the system size [20] and the relatively small size of the systems in our study did not allow to reliably investigate them.

Finally, we would like to note that non-equilibrium conformational activity should also have an important

effect on diffusion phenomena in biomembranes. On the scales shorter than the characteristic Saffman-Delbrück length of about one micrometer, lipid bilayers behave like two-dimensional fluids [22] and, therefore, a model with 2D diffusion is already applicable for them. Typically, protein inclusions make up to 40 percent of the membrane mass and most of such inclusions (e.g., ion pumps) are active and cyclically change their shapes. Based on our results, strong diffusion enhancement in presence of active inclusions can be expected for biomembranes.

## ACKNOWLEDGMENTS

Stimulating discussions with T. Ooshida and S. Komura are gratefully acknowledged. This work was supported by JSPS KAKENHI Grants No. JP19K03765 and No. JP19J00365 in Japan.

- 
- [1] P. Gaspard and R. Kapral, *Adv. Phys. X* **4**, 1602480 (2009).
  - [2] X.-L. Wu and A. Libchaber, *Phys. Rev. Lett.* **84**, 3017 (2000).
  - [3] C. Valeriani, M. Li, J. Novosel, J. Arlt, and D. Marenduzzo, *Soft Matter* **7**, 5228 (2011).
  - [4] K. Dey, *Angew. Chem. Int. Ed.* **58**, 2208 (2019).
  - [5] Self-propulsion may however perhaps still take place for some exceptionally rapid enzymes with microsecond turnover cycles, see [6].
  - [6] A.-Y. Jee, S. Dutta, Y.-K. Cho, T. Thlusty, and S. Granick, *Proc. Natl. Acad. Sci. USA* **115**, 14 (2018).
  - [7] T. Sakaue, R. Kapral, and A. S. Mikhailov, *Eur. Phys. J. B* **75** 381 (2010).
  - [8] S. Alonso and A. S. Mikhailov, *Phys. Rev. E* **79** 061906 (2009).
  - [9] A. S. Mikhailov and R. Kapral, *Proc. Natl. Acad. Sci. USA* **112** E3639 (2015).
  - [10] Y. Koyano, H. Kitahata, and A. S. Mikhailov, *Phys. Rev. E* **94**, 022416 (2016).
  - [11] A. S. Mikhailov, Y. Koyano, and H. Kitahata, *J. Phys. Soc. Jpn.* **86**, 101013 (2017).
  - [12] G. L. Hunter and E. R. Weeks, *Rep. Prog. Phys.* **75**, 066501 (2012).
  - [13] B. R. Parry, I. V. Surovtsev, M. T. Cabeen, C. S. O'Hern, C. S. Dufresne, and C. Jacobs-Wagner, *Cell* **156**, 183 (2014).
  - [14] F. Kogler, *Interactions of artificial molecular machines* (Diploma Thesis, Technical University, Berlin, 2009).
  - [15] H. Flechsig and A. S. Mikhailov, *J. R. Soc. Interface* **16**, 20190244 (2019).
  - [16] M. Dennison, R. Kapral, and H. Stark, *Soft Matter*, **13**, 3741 (2017).
  - [17] X. Chen, I. Weber, and R. W. Harrison, *J. Phys. Chem. B* **112**, 12073 (2008).
  - [18] A. Vendeville, D. Lariviere, and E. Fourmentin, *FEMS Microbiol. Rev.* **35**, 395 (2010).
  - [19] G. Nawrocki, A. Karaboga, Y. Sugita, and M. Feig, *Phys. Chem. Chem. Phys.* **21**, 876 (2019).
  - [20] B. Doliwa and A. Heuer, *Phys. Rev. E* **61**, 6898 (2000).
  - [21] T. Ooshida, S. Goto, T. Matsumoto, and M. Otsuki, *Phys. Rev. E* **94**, 022125 (2016).
  - [22] P. G. Saffman and M. Delbrück, *Proc. Natl. Acad. Sci. USA* **72**, 3111 (1975).